

RELATION BETWEEN POPULATION DENSITY AND TOPOLOGY IN POTABLE WATER DISTRIBUTION NETWORKS

Daniela Rojas¹, Cristina Moreno², and Juan Saldarriaga, M.Sc, M.ASCE³

¹Researcher, Water Supply and Sewer Systems Research Center (CIACUA), Universidad de los Andes, Bogotá, Colombia; e-mail: d.rojas1887@uniandes.edu.co

²Researcher, Water Supply and Sewer Systems Research Center (CIACUA), Universidad de los Andes, Bogotá, Colombia; e-mail: ac.morenob@uniandes.edu.co

³ Professor, Department of Environmental and Civil Engineering, Universidad de Los Andes, Bogotá; email: jsaldarr@uniandes.edu.co

ABSTRACT

It is well known that water supply constitutes one of the basic needs of every modern city, which depends on the number of inhabitants and its density. As population varies with time, building occupancy changes and uncertainty about the hydraulic behavior of Water Distribution Systems (WDS) arises. This paper presents a correlation analysis between the population density and the topology of potable WDS of two real networks with different geometric shapes, located in Colombia. The methodology proposed consists of three steps: i) Analysis of initial conditions related to population, system flows and geometry of each WDS; ii) Design of WDS under five scenarios of increases in population density, including the initial condition, using the Optimal Power Use of Surface (OPUS) methodology; iii) Analysis and verification of the networks' hydraulics and performances using pressure surfaces and pipe diameters, and calculation of efficiency indexes. Other analysis were carried out such as location of the geometric centroids of all designs, changes in water age and chlorine initial concentration in the tank, variations of cost per cubic meter of transported water and the fractality of each WDS. Main results showed that increases in population density did not necessarily lead to significant variations of the studied geometric parameters, that the reliability and energy efficiency indexes remained almost constant, and the variation of diameters was not uniform for all the pipe sections of the system.

INTRODUCTION

Throughout the history of human being, ancient communities tended to settle down near water resources in order to satisfy their main needs and fulfill their daily activities. However, great civilizations arose since they were able to understand the importance of water management for urban development by building water supply systems. Nowadays, WDS constitutes as an indispensable component in the infrastructure of every modern city, which topology and design depends on factors such as population number, population density and geographical location. Cities are constantly changing due to their economic, cultural, urban, social and political development, and as a result, non-uniform variations in demography occur, which may lead to uncertainties about the hydraulic capacity of the WDS. For that reason, the main objective of this paper is to analyze the effects that population density may have on the topology of a WDS.

Four real networks located in Colombia were selected using criteria of geometric shape and studied for this research, but only two study cases will be presented in this paper. Information of the characteristics of the networks and their actual supply flows were collected, and so, four scenarios of increases in flow rate were proposed to obtain networks with the same geometric

configuration but higher densification, i.e. higher water demand. After the creation of the study cases with five different flow demands (one real and four proposed), an optimization design methodology was used based in the use of Optimal Power Use of Surface (OPUS) (Saldarriaga et al. 2012) through the REDES research program (Saldarriaga et al. 2017). Indicators of reliability and energy efficiency were evaluated for the hydraulic analysis of the results obtained, and different network centroids (geometrical, topological, volume, mass) were created, using the coordinates of the tanks, nodes and pipes of each system. Additionally, chlorine concentration and water age were evaluated in each executed design in order to verify the impact of densification increase in water quality. Finally, costs per cubic meter were calculated using the equation defined by (Peinado and Saldarriaga 2016) and the fractality was verified with the methodology exposed by (Diao et al. 2017).

METHODOLOGY

Optimal Design of RDAP

As it was possible to use any other existent optimization methodology for this research, OPUS methodology was chosen as it has already been proved that it successfully generates results close to the optimal design, which implies obtaining good designs with minimal cost. This methodology allowed obtaining optimal designs with minimum cost with less iterations. This design procedure is based on the use of deterministic hydraulic principles, extracted from the analysis of flow distribution, and on an analysis of how optimal systems spend energy (Saldarriaga et al. 2012). Nevertheless, it is important to clarify that obtained results are not particularly dependent on the optimal design method efficiency.

Reliability and energy efficiency indexes

This study used the following indexes that assess the impact and response of a WDS under hydraulic and mechanical failures.

$$\begin{array}{l} \text{Resilience Index} \\ \text{(Todini 2000)} \end{array} \quad RI = \frac{\sum_{i=1}^{n_n} D_i (H_i - H_i^{(req)})}{\sum_{k=1}^{n_r} D_{out_k} H_k + \sum_{j=1}^{m_p} P_j / \gamma - \sum_{i=1}^{n_n} D_i H_i^{(req)}} \quad (1)$$

$$\begin{array}{l} \text{Modified Resilience Index} \\ \text{(Jayaram and Srinivasan 2008)} \end{array} \quad MRI = \frac{\sum_{i=1}^{n_n} D_i (H_i - H_i^{(req)})}{\sum_{i=1}^{n_n} D_i H_i^{(req)}} \quad (2)$$

$$\begin{array}{l} \text{Centralized Resilience Index} \\ \text{(Paez and Filion 2017)} \end{array} \quad CMRI = \frac{\sum_{i=1}^{n_n} D_i p_i}{\sum_{i=1}^{n_n} D_i p_{min}} - 1 \quad (3)$$

$$\begin{array}{l} \text{Specific Power Index} \\ \text{(Saldarriaga et al. 2010)} \end{array} \quad P_{PC} = \frac{\sum_{i=1}^{n_n} q_i (h_i - Z_{min})}{\sum_{i=1}^{n_e} Q_i (H_i - Z_{min})} * 100 \quad (4)$$

For Equations (1) to (4), D_i is the demand in node i ; H_i is the computed head in node i ; $H_i^{(req)}$ is the objective head in node i , D_{out_k} is the outflow from reservoir k ; H_k is the head in reservoir k ; P_j is the power of pump j , γ is the specific weight of water; n_n is the number of demand nodes and n_r is the number of reservoirs or water sources (may include some tanks). RI is based on the relationship between the resilience of a system and the amount of energy that it dissipates: if the dissipated energy is lower, the response capacity is greater because there is a bigger amount of available energy (Todini 2000). MRI is the ratio between available surplus power at demand nodes and required power (Paez and Filion 2017). $CMRI$ is the centralized version of the MRI and it is calculated by switching the model datum to get $\sum_{i=1}^{n_n} D_i z_i = 0$

(Paez and Fillion 2017). Finally, P_{PC} is a measure of the system-energy efficiency and it accounts for the percentage of total available energy that is used to meet demand. Larger values of P_{PC} indicate greater energy-efficiency of the network (Saldarriaga et al. 2010).

Geometric Indexes

The focus of this study is geometric, so four indexes that assess geometric attributes were created. Those indicators were calculated using the X and Y coordinates of each pair of nodes that limit each section of the n pipes of the system. The obtained values were called centroids and they were computed for volume, specific power, power and diameter parameters. The names given to the conceived indexes were: Volume Centroid (C_V) (Equation 5), Specific Power Centroid (CP_S) (Equation 6), Diameter Centroid (C_d) (Equation 7) and Power Centroid (C_P) (Equation 8).

$$C_V = \frac{\sum_{i=1}^{nt} V_i * D_{ist\ i}}{V_T} \quad (5) \quad CP_S = \frac{\sum_{i=1}^{nt} P_{Si} * D_{ist\ i}}{P_{ST}} \quad (6)$$

$$C_d = \frac{\sum_{i=1}^{nt} d_i * D_{ist\ i}}{\sum_{i=1}^{nt} d_i} \quad (7) \quad C_P = \frac{\sum_{i=1}^{nn} Q_D * h_i * D_{ist\ i}}{\sum_{i=1}^{nn} Q_D * h_i} \quad (8)$$

$$P_{Si} = q_i(h_{i,ini} - h_{i,fin}) \quad (9)$$

For Equations (5) to (8), V_i is the volume of the pipe i ; V_T is the total volume; P_{Si} is the specific power of the pipe i , calculated with the Equation (9) where q_i is the flow in the pipe i and $(h_{i,ini}, h_{i,fin})$ are the piezometric heights in the initial and final nodes of the pipe i respectively; P_{ST} is the total specific power; d_i is the diameter of the pipe i ; Q_D is the flow demanded in the node i ; h_i is the piezometric height in the node i ; n_t is the number of pipes and n_n is the number of demand nodes. Since Equation (8) involves nodes, C_P is calculated using each node X and Y coordinates. The distance term ($D_{ist\ i}$) in equations (5) to (7) refers to the pipe i centroid, which is calculated with Equations (10) and (11), for its X and Y coordinates respectively.

$$Dist_{(x_i)} = \frac{|C_{x_{ini}} - C_{x_{fin}}|}{2} + \min(C_{x_{ini}}, C_{x_{fin}}) \quad (10)$$

$$Dist_{(y_i)} = \frac{|C_{y_{ini}} - C_{y_{fin}}|}{2} + \min(C_{y_{ini}}, C_{y_{fin}}) \quad (11)$$

For Equations (10) and (11), $C_{x_{ini}}$, $C_{x_{fin}}$, $C_{y_{ini}}$ and $C_{y_{fin}}$ are the X and Y coordinates of the initial and final nodes of the pipe i respectively. Using the previously described expressions, the centroids were obtained for each network designed, for all the study cases and demand patterns, and finally, they were located in the respective network plane. Finally, it is important to note that the centroids were calculated with Colombian official coordinates.

Cost Equation

When designing a WDS the main objective is to set a diameter array that minimizes the cost function under hydraulic, commercial and constructive constrains. This issue can be modeled as a combinatorial optimization problem where the diameters of each network pipeline are the decision variables. The cost function proposed by (Peinado and Saldarriaga 2016) was adopted for this study. The cost equation employed (12) was updated from the original cost function by calculating present value to September 2017.

$$C = \sum_{i=1}^{NT} 0.00319 * L_i * D_i^{1.724} \quad (12)$$

C is the total cost in dollars (US\$), including the commercial value of the pipes and their installation, NT is the number of pipes and L_i and D_i are respectively, the length and diameter of pipe i .

Fractality

The fractality is defined as the existence of analogous patterns, in different scales, for the same network. This can be done considering an algorithm that can identify if the network is fractal or non-fractal was developed by means of the relation between the number of boxes needed to cover a network (N_B) and the size of the boxes (l_B) (Diao et al. 2017). Equation (13) is the fundamental scheme of fractal behavior for a network where, $N_{B(l_B)}$ is the number of boxes with size l_B , N_0 is the number of vertices in the network and d_B is the fractal dimension.

$$N_{B(l_B)} = N_0 l_B^{-d_B} \quad (13)$$

Linearizing Equation (13), $N_{B(l_B)}$ becomes the dependent variable of a linear function where the slope is represented by the fractal dimension and (l_B) is the independent variable. This can be done considering a network is fractal if the relationship between $\log_{10}(N_B)$ and $\log_{10}(l_B)$ is linear. The fitness between dependent and independent series is proved by means of the determination coefficient obtained after applying a linear regression analysis (Diao et al. 2017).

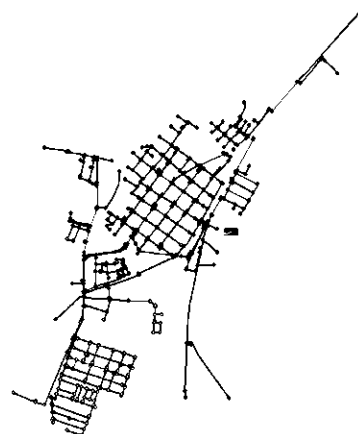
Considering that the tested designs generated the same geometry for the networks (even when population density increased), the fractal dimensions obtained were also the same. This considering that N_B and l_B series were modified by changing the value of the transported mass for each node (initially, it was considered that the mass was equal to 1 for all the network nodes). The modification leads to the formulation of two fractalities: Fractality 1 (F_1) and Fractality 2 (F_2). In the first case, the considered mass was the sum of flows that entered each node, and in the latter, this mass was the sum of flows multiplied by the HGL of the node. This calculation was proposed to verify changes in fractality of the network related with increases in mass.

STUDY CASES

The described methodology was applied to two real WDS with different geometric structures. The networks used as the study cases are located in Colombia, corresponding to the municipality of Bugalagrande in the region of Valle del Cauca and the Subsector 4 in Bogotá D.C (Sector 8). As it can be seen in Table 1, while Bugalagrande is a long network with branches and very low flows, Subsector 4 is a closed network with relatively short length and compact shape that seems to be more redundant.

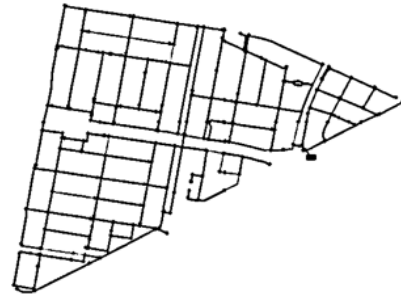
Table 1. Characteristics of the study cases

BUGALAGRANDE	
Number of Pipes	656
Number of Nodes	583
Number of Tanks	1
Total Length of Pipes [m]	31,000
Area Network [m ²]	2,550,000
Supply Flow [Lps]	52.47



SUBSECTOR 4

Number of Pipes	432
Number of Nodes	378
Number of Tanks	1
Total Length of Pipes [m]	21,000
Area Network [m ²]	1,097,071
Supply Flow [Lps]	110.39



For both studied networks, daily storage volume was calculated using the average-supply flow and the served population was estimated assuming a daily endowment of 100 liters per inhabitant. The population density was computed using the respective areas of the networks and five different optimal designs were executed with different population densities: Design 1 (D₁) represents the initial conditions with the population density calculated before; Design 2 (D₂) was executed with density values two times larger than D₁; Design 3 (D₃) with values three times larger; Design 4 (D₄) and Design 5 (D₅) with values four and eight times larger than the initial. Thus, flow rates were established for all five designs of each network, as shown in Table 2.

Table 2. Population densities and design flows.

	BUGALAGRANDE		SUBSECTOR 4	
	Density [Inhab/ha]	Flow Rate [lps]	Density [Inhab /ha]	Flow Rate [lps]
Design 1	97	52.47	473	110.39
Design 2	192	104.47	942	220.78
Design 3	287	156.63	1,413	331.18
Design 4	383	208.80	1,883	441.57
Design 5	765	417.45	3,760	883.14

RESULTS

For the study cases, the diameter pipes of the systems were calculated through the optimal design of the network, using both REDES and OPUS methodology. The results obtained were grouped into different ranges of diameter values in order to determine the distribution of pipe sizes of each network, given as the percentage of the relation between the number of pipes within a certain diameter range and the total number of pipes in the entire network. At the same time, the designs showed a constant increase in the network main-pipe system diameters.

The obtained hydraulic gradient surfaces presented similar behavior in both study cases as they were expected to vary slightly between the assorted designs, considering that OPUS guaranteed this because the methodology assigns the minimum pressure required at each node in order to meet demands at that point and downstream of it. Also, it was noted that the surfaces remained almost uniform, and that some small variations occurred due to the increase in diameters and flow rate, but these were eventually leveled with minimal pressures at the end of the network, as expected. These and other results of the analysis made are presented in the following sections, individually for both cases.

Bugalagrande Network

Designs executed for this network (Table 3) showed a constant increase in network main-pipe system diameters; however, it was observed that smaller diameters were more common because

of the supply distribution. In other words, as this network had many branches, the design methodology tended to favor minimum pressures and diameters.

Table 3. Percentage of existing diameters and maximum diameter in the Bugalagrande network.

DIAMETER RANGE	DESIGN 1	DESIGN 2	DESIGN 3	DESIGN 4	DESIGN 5
50mm – 100mm	92.3%	83.7%	80.6%	74.9%	70.2%
150mm – 300mm	7.2%	12.0%	12.6%	17.0%	20.2%
300mm – 600mm	0.5%	4.0%	6.0%	7.0%	8.1%
> 600mm	-	0.3%	0,8%	1.1%	1.5%
MAXIMUM DIAMETER (mm)	500	800	1,000	1,200	1,400

The resilience and energy efficiency indexes were calculated with Equations (1), (2), (3) and (4) and the obtained results are shown in Figure 1. Notice that indexes increased slightly until the third design because of the growth in the network main-pipes diameters, but then they started to decrease as smaller diameters were applied. Those reliability indexes demonstrate that Bugalagrande network had greater capacity to respond to possible failures. It also had an important percentage of available energy to supply the service because, as flow increased, available energy tried to remain constant Figure 2 shows pressure variations in the five executed designs, for some aleatory chosen nodes, evidencing minimal variations between designs.

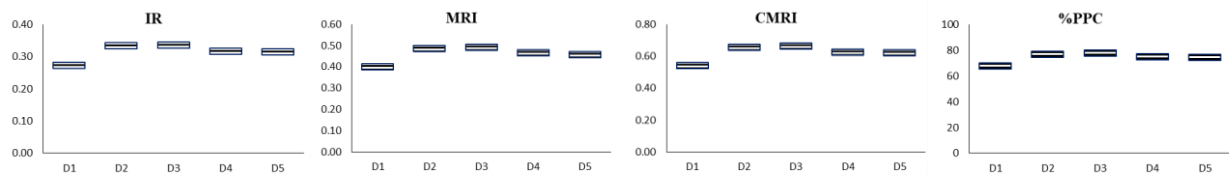


Figure 1. Resilience and energy efficiency indexes for the Bugalagrande network.

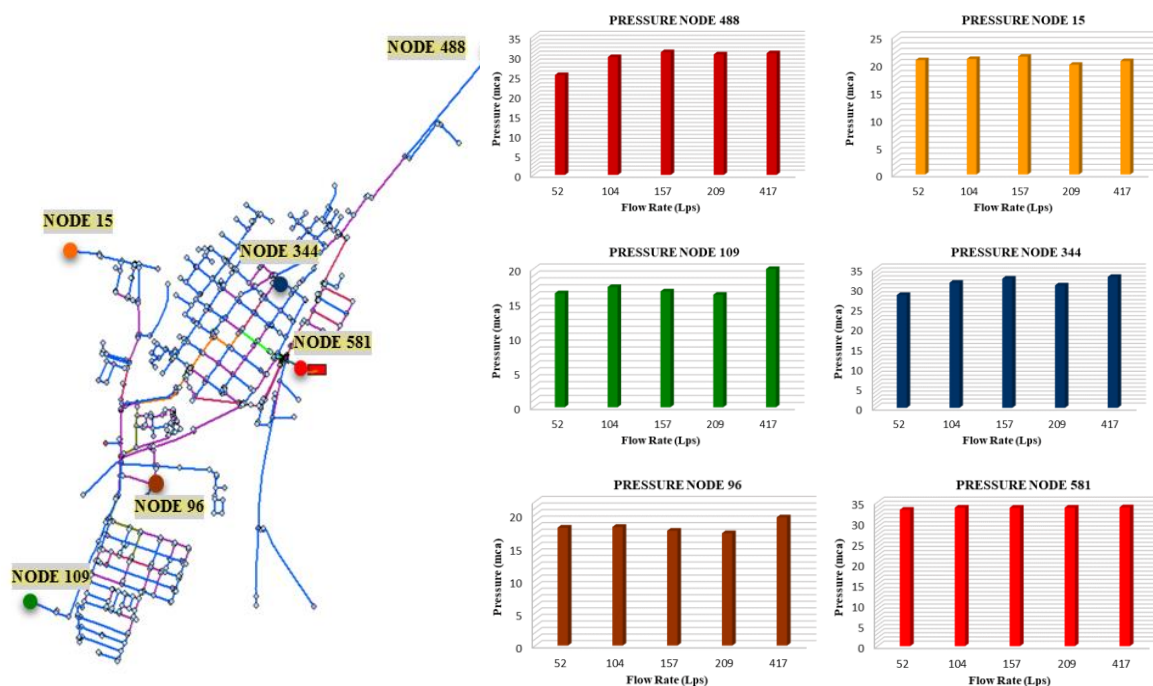


Figure 2. Pressure on nodes of the Bugalagrande network.

The centroids were calculated and they were placed in the map of the network by using the calculated coordinates. Table 4 shows the obtained coordinates of the four centroids of Bugalagrande network. The distances between each of the centroids of the five different designs moved within a range of 60 to 80 meters (they did not move more than one block between designs), which was possible to conclude that centroids were not directly affected by increases in densification, i.e. in the demanded flow. In this network, it was observed that Specific Power Centroid was in a coordinate closer to the tank (1102716.82, 957328.19) (See Figure 3 and Table 4).

Table 4. Coordinates of geometric centroids in the Bugalagrande network.

	VOLUME CENTROID (m)		SPECIFIC POWER CENTROID (m)		DIAMETER CENTROID (m)		POWER CENTROID (m)	
	C _x	C _y	C _x	C _y	C _x	C _y	C _x	C _y
D1	1102228.92	957225.38	1102535.81	957560.13	1102218.58	957243.73		
D2	1102285.95	957286.46	1102528.28	957570.25	1102246.24	957280.20		
D3	1102304.10	957309.58	1102529.70	957551.90	1102257.50	957296.03	1102238.08	957349.08
D4	1102305.48	957305.97	1102529.20	957601.42	1102262.92	957299.08		
D5	1102251.91	957242.51	1102519.04	957585.05	1102227.55	957254.64		

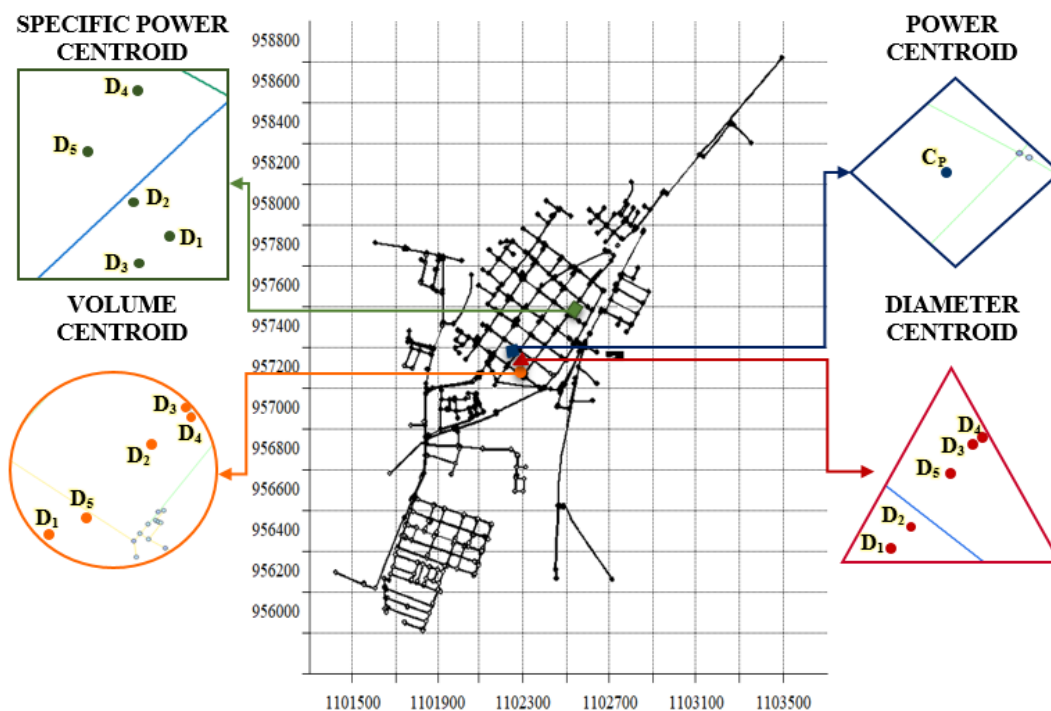


Figure 3. Localization of Centroids in the Bugalagrande network. ● Volume Centroid; ■ Specific Power Centroid; ◆ Power Centroid; ▲ Diameter Centroid.

Sector 8 - Subsector 4 Network

This network had a triangular shape and it presented a lot of redundancy; therefore, obtained designs include smaller diameters and constant increases, as can be consulted on Table 5. The pressures surface was leveled with respect to defined demand and it presented high pressures due to the network flat topography.

Table 5. Percentage of existing diameters and maximum diameter in the Subsector 4 network

DIAMETER RANGE	DESIGN 1	DESIGN 2	DESIGN 3	DESIGN 4	DESIGN 5
50mm – 100mm	84.0%	81.0%	80.5%	80.0%	75.0%
150mm – 300mm	16.0%	19.0%	16.5%	16.0%	15.0%
300mm – 600mm	-	-	3%	4.0%	10.0%
MAXIMUM DIAMETER (mm)	250	300	350	400	500

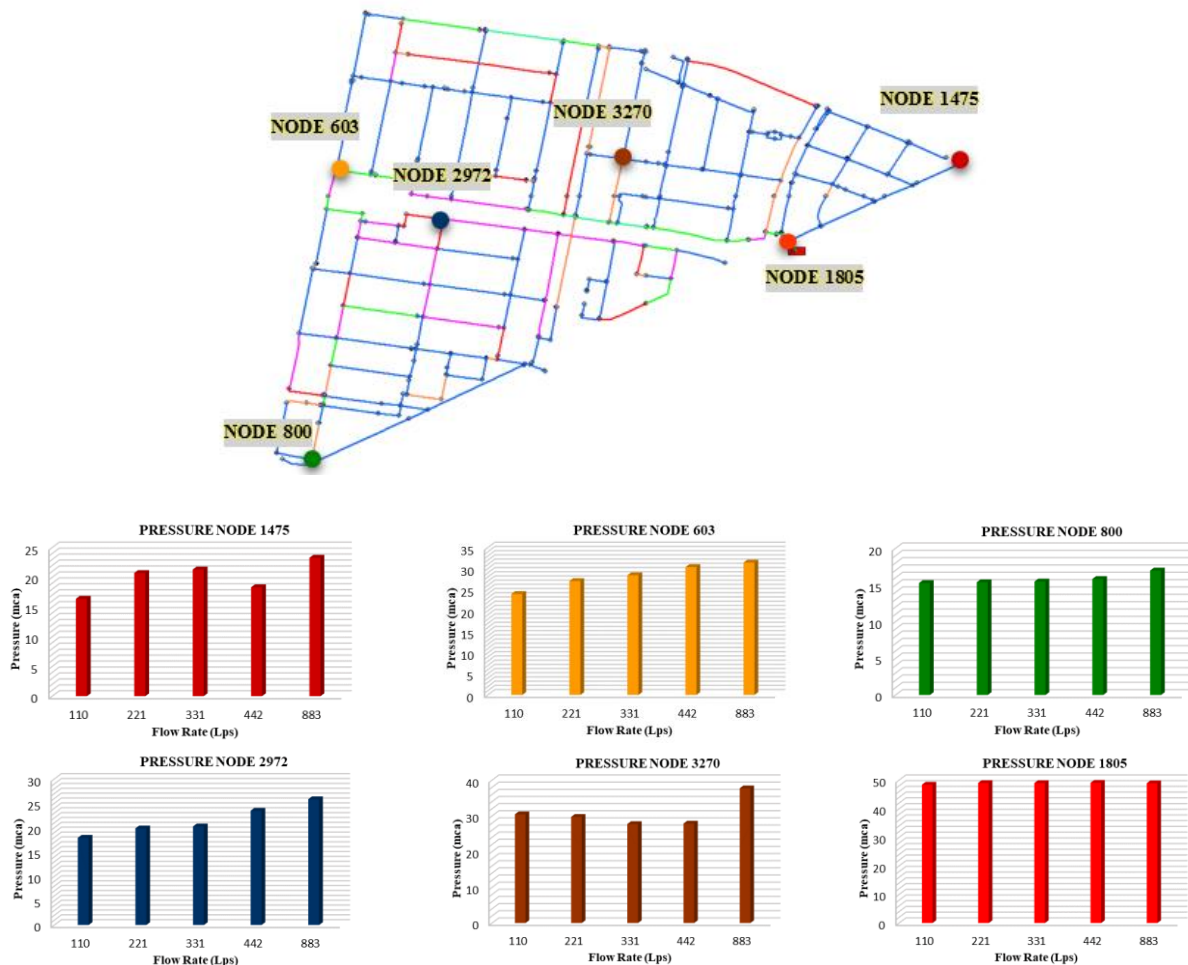


Figure 4. Pressure on nodes of the Subsector 4 network.

As can be seen on Figure 5, resilience and energy efficiency indexes for analyzed network were low, which implied that available energy and response to possible failures were also low. These variations were 20% maximum so that they did not generate significant changes on the energy efficiency of the system.

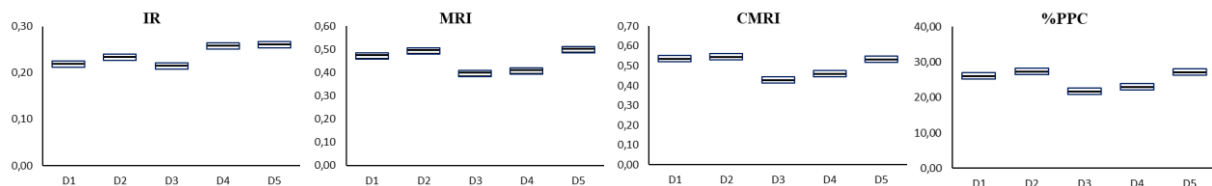


Figure 5. Resilience and energy efficiency indexes for the Subsector 4 network

Table 6. Coordinates of geometric centroids in the Subsector 4 network

	VOLUME		SPECIFIC POWER		DIAMETER		POWER	
	CENTROID (m)		CENTROID (m)		CENTROID (m)		CENTROID (m)	
	C _x	C _y						
D1	102748.33	109957.21	102995.97	109929.75	102802.68	109937.57		
D2	102752.96	109943.60	102923.76	109945.96	102807.20	109922.69		
D3	102757.05	109930.10	102902.24	109952.63	102810.49	109913.26	102767.62	109969.44
D4	102762.23	109931.34	102920.52	109951.84	102813.69	109915.09		
D5	102760.17	109939.68	102898.57	109950.46	102812.89	109914.18		

The calculated centroids were located towards the central part of the network, except for the Specific Power Centroid which was closer to the tank (see Table 6 and Figure 6). The volume and power centroids had a maximum variation of 40 meters, and the specific power centroids were separated by a maximum of 100 meters, corresponding to greatest increase in population density.

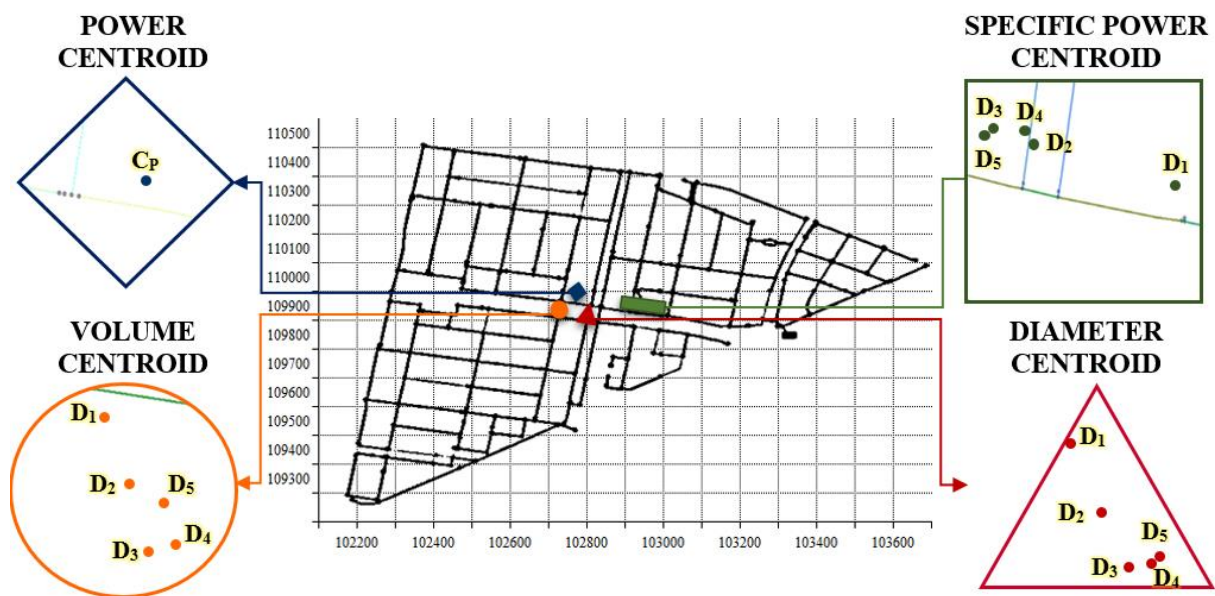


Figure 6. Localization of Centroids in the Subsector 4 network. ● Volume Centroid; ■ Specific Power Centroid; ◆ Power Centroid; ▲ Diameter Centroid.

Chlorine concentration analysis was carried out by using REDES. An initial tank concentration of 2 mg/L was considered in order to evaluate the minimum concentration at any node of the network. It is important to mention that, for all designs, the reported concentrations did not necessarily correspond to the same node or to the farthest node of the network. The procedure allowed verifying that increases in densification and consequently, in supply flow, generated bigger requirements of chlorine initial concentration in the tank, so the minimum concentration required could be guaranteed for each node. Nonetheless, the chlorine concentration in the system decayed as densification increased (see Table 7).

On the other hand, the fractal dimensions given in Table 7 did not present notable changes as population density increased. The variation of the obtained data was evaluated as percentage of the variation between the bigger and the smallest dimension among all same-network designs, for the both computed fractalities. In the Bugalagrande network, there was a variation of 1.59% and 1.48% for F1 and F2, respectively. In Subsector 4, the largest variations were obtained and they were in the order of 3% for both calculated fractal dimensions.

Table 7. Fractality and Chlorine concentration.

		BUGALAGRANDE			SUBSECTOR 4		
		Factality		Chlorine	Factality		Chlorine
		F ₁	F ₂	(mg/L)	F ₁	F ₂	(mg/L)
D1		0.959	0.958	1.68	0.991	0.991	1.64
	R²	0.98	0.97		0.99	0.99	
D2		0.956	0.951	1.52	0.968	0.965	1.25
	R²	0.99	0.99		0.98	0.99	
D3		0.954	0.951	1.35	0.993	0.989	1.19
	R²	0.99	0.99		0.98	0.99	
D4		0.961	0.951	1.15	0.981	0.979	1.13
	R²	0.99	0.99		0.99	1.00	
D5		0.946	0.944	0.74	0.996	0.993	0.93
	R²	0.98	0.98		0.99	0.99	

Additionally, REDES was useful to determine the water age by employing the values of the geometrically most distant node from the tank. There was a decrease in water age as population density and water demands in the nodes increased, which reduced the time the water travel through the whole system.

Finally, the analysis for costs per transported cubic meter were calculated using Equation (12) and presented in Table 8. The costs varied depending on the real cost equation and they were only calculated with the objective of verifying the effect of increasing the population density. It was also possible to conclude that costs were notably reduced when WDS transport greater flows, which indicates that is cheaper to move water in a densified network than in a longer network with fewer inhabitants per area.

Table 8. Age of water for the geometrically most distant node from the tank and cost per cubic meter moved

		BUGALAGRANDE		SUBSECTOR 4	
		Water Age	COST	Water Age	COST (US\$/m ³)
		(seg)	(US\$/m ³)	(seg)	
D1		10106	\$ 0.622	10386	\$ 0.270
D2		9606	\$ 0.568	8858	\$ 0.106
D3		8427	\$ 0.504	3080	\$ 0.081
D4		5983	\$ 0.474	2672	\$ 0.073
D5		4653	\$ 0.241	2174	\$ 0.055

CONCLUSIONS

The evaluation methodology through geometric centroids showed that topological changes of networks were independent from population density; this fact was verified through the geometric centroids location in the network plans. The obtained centroids moved distances no greater than 100 meters whenever population density increased, which implied that they did not move more than a block. This result was considered unusual because study networks had more than 35 km in length and the population densities assigned were relatively high.

The reliability and energy efficiency indexes showed small variations that were not seen as relevant in this study because the indexes remained relatively constant considering changes in densification. This result indicated that the available energy required to supply services was maintained despite population density changes.

Changes in the diameter in the networks' main pipe routes and pressure increases in areas near to the supply tank occurred due to an increase in population density. OPUS design methodology was used considering this and pressures were leveled throughout the networks in order to deliver the minimum pressure required for each case and, as a result, the minimum design diameter. Regarding water quality, it was possible to verify that a higher chlorine initial concentration was required in tanks and that water age decreased when the network is densified.

The fractality was verified for all the study cases through REDES and very small execution times were obtained since the study was carried out for relatively small networks. In both networks, fractality was close to 1.0 with a good correlation coefficient R2.

REFERENCES

Diao, K., Butler, D., Ulanicki, B. (2017). "Fractality in water distribution networks". Computing and Control for the Water Industry, Sheffield, 5th – 7th September 2017. <https://doi.org/10.15131/shef.data.5364151.v1>

Gheisi, A., Forsyth, M., Naser, G. (2016). "Water Distribution Systems Reliability: A Review of Research Literature". Journal of Water Resources Planning and Management, 142(11). [https://doi.org/10.1061/\(ASCE\)WR.1943-5452.0000690](https://doi.org/10.1061/(ASCE)WR.1943-5452.0000690)

Jayaram, N., Srinivasan, K. (2008). "Performance-based optimal design and rehabilitation of water distribution networks using life cycle costing". Water Resources Research, 44(1), 1–15. <https://doi.org/10.1029/2006WR005316>

Paez, D., Fillion, Y. (2017). "Generation and Validation of Synthetic WDS Case Studies Using Graph Theory and Reliability Indexes". Procedia Engineering, 186, 143–151. <https://doi.org/10.1016/j.proeng.2017.03.220>

Peinado, C. D., Saldarriaga, J. (2016). "Ecuaciones de costo para el diseño optimizado de redes de agua potable y alcantarillado" (Tesis de Maestría no publicada). Universidad de los Andes. Bogotá.

Saldarriaga, J., Hernández, F., Escovar, M. A., Páez, D. A. (2012). "Superficie de uso óptimo de potencia para el diseño de redes de distribución de agua potable". XXV Congreso Latinoamericano de Hidráulica San José, Costa Rica, 2012. (ISBN 978-9968-933-06-3).

Saldarriaga, J., López, L., Páez, D., Luna, D., González, S. (2017). "Optimized Design of Water Distribution Networks (Software REDES)". XV Seminario Iberoamericano de Redes de Agua y Drenaje, SEREA2017. Universidad de los Andes. Bogotá.

Saldarriaga, J., Mendoza, F. (2010). "Diseño optimizado de Redes de Distribución de Agua Potable Incluyendo Análisis de Costo Mínimo versus Resiliencia de la Red". XXIV Congreso Latinoamericano de Hidráulica Selección de Trabajos Punta Del Este, Uruguay, 2010. (ISBN 978-92-9089-184-0).

Saldarriaga, J., Ochoa, S., Moreno, M., Romero, N., Cortés, Ó. (2010). "Prioritized Renewal of Water Distribution Networks Using Unitary Power Concept". *Urban Water Journal*, 7(2), 121–140. <https://doi.org/10.1080/15730620903447621>

Saldarriaga, J., Páez, D., Cuero, P., León, N. (2012). "Optimal power use surface for design of water distribution systems". 14th International Water Distribution Systems Analysis Conference World Environmental & Water Resources Congress 2012: Crossing Boundaries, Adelaide, Australia. (ISBN 9780784412312).

Todini, E. (2000). "Looped water distribution networks design using a resilience index based heuristic approach". *Urban Water Journal*, 2(2), 115–122. [https://doi.org/10.1016/S1462-0758\(00\)00049-2](https://doi.org/10.1016/S1462-0758(00)00049-2)